Published in final edited form as:
Mol Pharm. 2010 April 5; 7(2): 442–455. doi:10.1021/mp9002255.

pH-responsive polymeric siRNA carriers sensitize multidrug resistant ovarian cancer cells to doxorubicin via knockdown of polo-like kinase 1

Danielle S.W. Benoit[†], **Scott M. Henry**[†], **Andrew D. Shubin**, **Allan S. Hoffman**, and **Patrick S. Stayton**[*]
Department of Bioengineering, University of Washington, Seattle WA 98195

Abstract

Small interfering RNA (siRNA)-based therapies have great potential for the treatment of debilitating diseases such as cancer, but an effective delivery strategy for siRNA is elusive. Here, pH-responsive complexes were developed for the delivery of siRNA in order to sensitize drug-resistant ovarian cancer cells (NCI/ADR-RES) to doxorubicin. The electrostatic complexes consisted of a cationic micelle used as a nucleating core, siRNA, and a pH-responsive endosomolytic polymer. Cationic micelles were formed from diblock copolymers of dimethylaminoethyl methacrylate (pDMAEMA) and butyl methacrylate (pDbB). The hydrophobic butyl core mediated micelle formation while the positively-charged pDMAEMA corona enabled siRNA condensation. To enhance cytosolic delivery through endosomal release, a pH-responsive copolymer of poly(styrene-*alt*-maleic anhydride) (pSMA) was electrostatically complexed with the positively-charged siRNA/micelle to form a ternary complex. Complexes exhibited size (30–105 nm) and charge (slightly positive) properties important for endocytosis and were found to be non-cytotoxic and mediate uptake in >70% of ovarian cancer cells after 1 hour of incubation. The pH-responsive ternary complexes were used to deliver siRNA against polo-like kinase 1 (*plk1*), a gene upregulated in many cancers and responsible for cell cycle progression, to ovarian cancer cell lines. Treatment resulted in ~50% reduction of *plk1* gene expression in the drug-resistant NCI/ADR-RES ovarian cancer cell model and in the drug-sensitive parental cell line, OVCAR8. This knockdown functionally sensitized NCI/ADR-RES cells to doxorubicin at levels similar to OVCAR8. Sensitization occurred through a p53 signaling pathway, as indicated by caspase 3/7 upregulation following *plk1* knockdown and doxorubicin treatment, and this effect could be abrogated using a p53 inhibitor. To demonstrate the potential for dual delivery from this polymer system, micelle cores were subsequently loaded with doxorubicin and utilized in ternary complexes to achieve cell sensitization through simultaneous siRNA and drug delivery from a single carrier. These results show knockdown of *plk1* results in sensitization of multidrug resistant cells to doxorubicin, and this combination of gene silencing and small molecule drug delivery may prove useful to achieve potent therapeutic effects.

Keywords

siRNA delivery; pH-responsive polymers; multidrug resistance; polo-like kinase 1; doxorubicin; NCI/ADR-RES; pSMA

[*]Corresponding Author: Patrick S. Stayton, Ph.D., University of Washington, Department of Bioengineering, Box 355061, Seattle, WA 98195, Tel: (206) 685.8148, Fax: (206) 685.8526, stayton@u.washington.edu.
[†]Equally contributing authors

Introduction

Small interfering RNA (siRNA) offers sequence-specific, post-transcriptional silencing of genes and is particularly attractive for the treatment of diseases distinguished by altered patterns of gene expression (e.g., cancer) [1, 2]. A number of cancer genes have been identified that regulate apoptosis, proliferation, cell signaling, and multidrug resistance. Selective knockdown of one or several of these genes could be an effective strategy for anti-cancer treatment alone or in combination with chemotherapeutic drugs. Promising siRNA targets include anti-apoptotic genes such as *bcl2* [3], drug resistance genes such as *mdr1* [4, 5], drug-sensitizing genes such as *rad51/50* [6] and others[2, 7–10]. Polo-like kinase 1 (*plk1*) plays a critical regulatory role in cell cycle progression, is over-expressed in a broad range of tumors, and has been implicated in tumorigenesis and progression[11, 12]. Overexpression of *plk1* is sufficient for malignant transformation of NIH3T3 cells[13], prevents apoptosis in response to DNA damage [14, 15], and is linked to poor patient survival rates[16–18]. *Plk1* acts by inhibiting the pro-apoptotic activity of tumor-suppressor protein p53, increasing the resistance of affected cells to genetic damage caused by many anti-neoplastic agents[11, 19]. Studies using small-molecule kinase inhibitors have shown that inhibition of *plk1* increases the sensitivity of tumor cells to chemotherapeutics, but the clinical use of such drugs is compromised by off-target kinase inhibition[12, 20]. Knockdown of *plk1* using siRNA has been shown to cause cell-cycle arrest and apoptosis in cancer cells, but not in normal cell lines[21–23]. Given the role of *plk1* in p53 suppression, delivery of siRNA against *plk1* in combination with chemotherapeutics is likely to increase the sensitivity of targeted cells to chemotherapeutics, producing a synergistic increase in tumor-cell apoptosis beyond the levels obtained by *plk1* knockdown alone. This effect could have significant utility, particularly in the treatment of multidrug resistant cancers. In fact, previous studies have examined the delivery of siRNA against *rad51*, *bcl2/xl*, *xIAP*, glutaredoxin, hypoxia inducible factor-1 α, Src kinase, Kruppel-like factor 6, erythroid-2-related factor 2, and *mdr1* to increase the sensitivity of cancer cells or multidrug resistant cancer cells to traditional chemotherapeutics [3–5, 8, 24–31]. However, efficient and safe delivery of therapeutic siRNA to the cytoplasm of targeted cells remains a fundamental limitation to its development as a clinical therapy.

Typically, synthetic siRNA is delivered using carriers that electrostatically complex siRNA, protecting the siRNA from nuclease activity and increasing uptake through interactions with the negatively-charged cell membrane. The predominant route of cellular entry for such complexes is endocytosis, which leads to enzymatic degradation in the lysosome and/or recycling and extracellular clearance. Consequently, much work has focused on carriers that mediate cytoplasmic delivery of nucleic acids by enhancing endosomal escape. Many cationic polymer carriers, such as poly(ethylenimine) (PEI), mediate endosomal escape by osmotic rupture of the endosome through the ‘proton sponge effect’32–40. Other carriers that become membrane destabilizing in the endosome have also been widely explored, including cationic or fusogenic lipids such as dioleoyloxy-3-trimethylammonium propane (DOTAP), viral vectors, fusogenic proteins, and synthetic peptides 41–47. These pH-responsive carriers undergo a hydrophilic-to-hydrophobic transition as the pH changes from physiologic (~7.4) to acidic (~6.6–5.8) within the endosomal-lysosomal pathway, enabling membrane interaction and destabilization. However, the clinical application of these carriers is limited by concerns of tumorgenicity, immunogenicity, and notable toxicity associated with cationic carriers 48–50.

As an alternative approach, pH-responsive, membrane-destabilizing synthetic polymers have been investigated to enhance the cytoplasmic delivery of therapeutic macromolecules 51–54. These are amphiphilic polymers that contain a critical balance of acidic carboxyl groups and hydrophobic moieties. The carboxylate ions of these polymers become protonated at

endosomal pH values, and the polymers undergo a change from a hydrophilic, biologically inert state to a hydrophobic and membrane-destabilizing one. In particular, the polymer poly(propylacrylic acid) [51–53] and alkylamine derivatives of poly(styrene-*alt*-maleic anhydride) (pSMA) [55] have received recent attention for their pH-responsive behaviors. Unlike carriers based on viral peptides or cationic polymers, anionic polymers are non-immunogenic and non-toxic[56–58].

To address the limitations of therapeutic siRNA delivery, a polymeric delivery system is described that enhances intracellular delivery of siRNA. The polymer complexes consist of three basic components: (1) cationic micelles employed as nucleation cores of the complexes (2) siRNA and (3) anionic, pH-sensitive pSMA polymers that mediate endosomal escape. The micelles are formed from amphiphilic diblock poly(dimethylaminoethyl methacrylate-block-butyl methacrylate) copolymers that self-assemble to form micelles with hydrophobic cores and cationic coronas. These micelles electrostatically complex siRNA and pH-responsive alkylamine derivatives of pSMA, forming a ternary complex. The micelles employed herein are also capable of loading chemotherapeutics such as doxorubicin, offering the potential for concomitant gene and chemical therapy from a single carrier [59, 60]. Ternary complexes formulated with siRNA against *plk1* achieve significant knockdown in drug-sensitive and multidrug resistant ovarian cancer cells with dependence of knockdown on micelle and ternary complex formulation and siRNA dose. Knockdown of *plk1* in these cell types significantly increases their susceptibility to doxorubicin. Importantly, multidrug resistant cells with reduced *plk1* exhibit the same sensitivity to doxorubicin as drug-sensitive cells with normal *plk1* levels. Caspase 3/7 is upregulated in multidrug resistant cells in response to *plk1* knockdown and doxorubicin treatment, and exposure to a p53 inhibitor (pifithrin α) resulted in restoration of the doxorubicin-resistant phenotype. Both caspase upregulation and reversion to the doxorubicin-resistant phenotype indicate that effects of *plk1* knockdown are specific to the p53 signaling mechanism. Although this polymeric delivery system is described in the context of cancer therapy, it is important to note that it is highly modular and can be employed in other therapeutic strategies simply by changing the sequence of the therapeutic siRNA or drug without requiring further optimization of the other components.

2. Materials and Methods

2.1 Materials and Instrumentation

All chemicals were obtained from Sigma-Aldrich and used without purification unless otherwise noted. Dimethylaminoethyl methacrylate (DMAEMA), butyl methacrylate (BMA), and styrene were purified by vacuum distillation. The free-radical sources, 2,2-azobisisobutyronitrile (AIBN) and 2,2'-Azobis(4-methoxy-2.4-dimethyl valeronitrile) (V-70, Wako) were recrystallized from methanol.

The polymers in this work were characterized by gel permeation chromatography using three Tosoh TSK-GEL columns (TSK-α3000, α3000, α4000) connected in series to a Viscotek GPCmax VE2001 and Viscotek RI and UV detectors (VE3580 and VE3210 respectively) (Viscotek, Houston Tx). The mobile phase was HPLC-grade DMF containing 0.1 wt% LiBr. Molecular weight distributions were determined relative to a series of poly(methyl methacrylate) standards.

2.2 Ternary carrier polymer synthesis

The diblock polymer poly(dimethylaminoethyl methacrylate-block-butyl methacrylate) (pDbB) was obtained from a two-step reversible addition fragmentation chain transfer (RAFT) polymerization using a trithiocarbonate chain transfer agent (CTA), dodecyl

cyanovaleric trithiocarbonate (DCT), synthesized as previously described [61]. In the first step, a poly(dimethlyaminoethyl methacrylate) (pDMAEMA) macroCTA was obtained by polymerizing DMAEMA at a $[CTA_o]/[I_o]$ ratio of 30:1 (AIBN radical source) and a $[CTA_o]/[M_o]$ ratio of 1:200 (30 wt% in *N,N'*-dimethylformamide (DMF), 60 °C for 6 hours, nitrogen atmosphere). pDMAEMA was isolated by precipitation in an 80/20 v/v pentane/ether mixture, followed by repeated cycles of dissolution in ether and precipitation in pentane, and dried under vacuum. The molecular weight (M_n) and polydispersity were 7,300 g/mol and 1.2, respectively. In the second step, pDMAEMA was used as a macroCTA for the polymerization of butyl methacrylate ($[CTA_o]/[I_o]$=20:1 (V-70 radical source), $[CTA_o]/[M_o]$=1:70, 60 wt% DMF, 30 °C for 12 hours, nitrogen atmosphere). pDbB was isolated by precipitation in 80/20 v/v pentane/ether mixture, followed by repeated cycles of dissolution in ether and precipitation in pentane, and dried under vacuum. The molecular weight (M_n) and polydispersity of the block copolymer were 9,400 g/mol and 1.2 respectively.

Alkylamine derivatives of poly(styrene-*alt*-maleic anhydride) (pSMA) were previously developed and thoroughly characterized with respect to membrane disruption in response to lowered pH values characteristic of the endosomal/lysosomal pathway[55]. Both pSMA molecular weight and extent and type of alkylamine modification impacts the pH-responsiveness 55. Based on these results, pSMA of molecular weight 48,500 g/mol (M_n) was synthesized by RAFT polymerization (polydispersity = 1.3) and derivatized with 60% pentylamine. Briefly, equimolar amounts (0.02 mol) styrene and maleic anhydride were polymerized using a $[CTA_o]/[I_o]$ ratio of 10:1 (AIBN radical source), and a $[CTA_o]/[M_o]$ ratio of 1:580 (50 wt% dioxane, 60 °C, 22 hours, nitrogen atmosphere). 4-cyanopentanoic acid dithiobenzoate (CTP) was employed as the RAFT agent (synthesized as previously described 62). pSMA was isolated by precipitation in ethyl ether, and subsequent alkylamine modification and hydrolysis were performed as described elsewhere 55.

2.3 Ternary complex formation and characterization

Cationic micelles of the pDbB copolymers were obtained by a solvent displacement method. 23 mg of pDbB was dissolved in 3.7 ml MeOH. An equivalent volume of deionized H_2O was added at 12.2 μL/min, such that the original solvent was diluted 50% with water after 5 hours. The solvent mixture was then transferred to a Slide-A-Lyzer dialysis cassette (MWCO = 3,500, Pierce) and dialyzed against deionized H_2O for 24 hours. The solutions were then filtered through a 0.2 μm syringe filter and lyophilized. The lyophilized solids were resuspended in PBS pH 7.4 at a concentration of 1 mg/ml for subsequent knockdown experiments.

To formulate the ternary complexes, the appropriate amount of siRNA was added to a solution of pDbB micelles in PBS at pH 7.4 in order to achieve a desired micellar charge ratio (+/−), over a range of 8:1 to 2:1. The micelle charge ratio is the ratio of positively-charged pDMAEMA residues to the number of phosphate groups present in the siRNA backbone, assuming 50% protonation of the pDMAEMA residues at pH 7.4 based on the pKa. After 15 minutes of complexation, a solution of pSMA in PBS at pH 7.4 was added to the binary siRNA/micelle complexes to achieve a desired overall charge ratio (+/−), over a range of 8:1 to 1:3:1, accounting for the additional negative charges from the carboxylate groups in the pSMA polymer. The degree of protonation of the pSMA polymers was determined from pKa data previously published [55]. Ternary complexes were characterized for size and zeta potential using a ZetaPALS detector (Brookhaven Instruments Corporation, Holtsville, NY, 15 mW laser, incident beam = 676 nm) in Dulbecco's phosphate buffered saline (without calcium and magnesium). Correlation functions were collected at a scattering angle of 90°, and particle sizes were calculated using the viscosity and refractive index of water at 25 °C. Particle sizes are expressed as the number average assuming a log-normal distribution. Average electrophoretic mobilities were measured at 25 °C using the ZetaPALS

zeta potential analysis software, and zeta potentials were calculated using the Smoluchowsky model for aqueous suspensions.

2.4 Ternary complex cytotoxicity

Ternary complex cytotoxicity was determined using a lactate dehydrogenase (LDH) cytotoxicity detection kit (Roche). NCI-ADR/RES cells were seeded in 96-well plates at a density of 25,000 cells/cm^2. NCI-ADR/RES is a multidrug resistant ovarian cancer cell line derived from OVCAR8 cells, obtained from the NCI repository, and maintained in RPMI 1640 media + 10% fetal bovine serum and 1% penicillin-streptomyocin (Invitrogen). After 24 hours incubation, ternary complexes of varying micelle and overall charge ratios were added to the cells at a final concentration of 25 nM siRNA (control siRNA #1, Ambion) in serum-free conditions. After 4 hours incubation, serum was added to the wells at 10% of the final volume. After 24 hours, the cells were rinsed twice with PBS and lysed (100 μL/well, 20 mM Tris-HCl, pH 7.5, 150 mM NaCl, 1 mM EDTA, 1 mM EGTA, 1% TritonX-100, 2.5 mM sodium pyrophosphate, 1 mM β-glycerophosphate, 1 mM sodium orthovanadate) for 1 hour at 4 °C. The cell lysate was diluted 1:5 in PBS and quantified for lactate dehydrogenase (LDH) according to the manufacturer's specifications (Roche Cytotoxicity Detection Kit (LDH)).

2.5 Ternary complex mediated siRNA uptake and *plk1* knockdown and sensitization towards doxorubicin

Intracellular uptake of siRNA ternary complexes was measured using flow cytometry (Becton Dickinson LSR bench top analyzer). NCI/ADR-RES were seeded at 25,000 cells/cm^2 and allowed to adhere overnight. FAM-labeled siRNA (Ambion) was incorporated into ternary complexes at various micellar and overall charge ratios, and added to the plated cells at a final siRNA concentration of 25 nM in serum-free conditions. After incubation with the complexes for 1 hour, the cells were trypsinized and resuspended in PBS with 0.5% BSA and 0.01% trypan blue. Trypan blue was utilized as previously described to quench extracellular fluorescence, enabling the discrimination of ternary complexes that had been endocytosed[63]. 10,000 cells were analyzed per sample and fluorescence gating was determined using samples receiving no treatment, treated with naked siRNA (no carrier), and using a commercially available carrier, HiPerFect (Qiagen).

The efficacy of the ternary complexes for siRNA delivery was evaluated using RT-PCR to screen for the most effective complex formulations. OVCAR8 or NCI/ADR-RES cells were plated in 24-well plates (25,000 cells/cm^2). After 24 hours, ternary complexes (micellar charge ratio of 8:1 and overall charge ratios of 4:1, 2:1, and 1:3:1 as well as micellar charge ratios of 8:1, 4:1, and 2:1 and overall charge ratio of 1:3:1) were added to the cells at a final *plk1* siRNA (Ambion) concentration of 25 nM in serum-free media (100 μL volume). After 4 hours, serum was added to 10% of the final volume. As a positive control, parallel knockdown experiments were run using the commercially available siRNA carrier, HiPerFect (Qiagen), following manufacturer's conditions. The extent of siRNA-mediated *plk1* mRNA reduction was assessed after 48 hours. Total RNA was isolated using Qiagen's Qiashredder and RNeasy Mini Kit. Residual DNA in the samples was digested (RNase-Free DNase Set, Qiagen) and RNA was quantified using absorbance at 260 nm. Reverse transcription was performed using the Omniscript RT kit (Qiagen). A total of 10 ng RNA sample was used for cDNA synthesis and PCR was conducted using the ABI Sequence Detection System 7000 using predesigned primer and probe sets (Assays on Demand, Applied Biosystems) for *plk1* and β-*actin* as the housekeeping gene. Comparative threshold cycle (C_T) analysis was used to quantify *plk1* normalized to β-*actin* and relative to expression of untreated cells. Following analysis to determine the most potent ternary

complex formulation for siRNA delivery, gene knockdown was analyzed in response to siRNA dose (5, 10, 25, and 50 nM) using RT-PCR as described above.

To determine the sensitization towards doxorubicin, cells (OVCAR8 and NCI/ADR-RES) were seeded at 25,000 cells/cm^2 in 96-well, clear bottom, black plates and allowed to adhere overnight. Ternary complexes at 8:1 micelle charge ratio and 2:1 overall charge ratio, determined to be the most efficacious formulation for gene knockdown, were added to the cells at a final *plk1* siRNA (Ambion) concentration of 25 nM in serum-free media. After 4 hours, serum was added to 10% of the final volume. After 48 hours, doxorubicin was added at various concentrations (0, 0.1, 0.5, 1, 5, 10, 50, and 100 μg/ml). Metabolic activity of the treated cells, which is an indirect measure of the number of living cells, of the treated cells was analyzed after an additional 24 hours. A 10 vol% solution of AlamarBlue in media was added to cells. Active mitochondria convert resazurin, the active ingredient in AlamarBlue, to resorufin, a fluorescent molecule. After 4 hours of incubation, the media/AlamarBlue solution was analyzed for fluorescence with a plate reader (Tecan Safire 2) and % cell viability and IC_{50} (inhibitory concentration to 50% of the population) were determined by comparing fluorescence of samples to controls.

Caspase 3/7 activation was measured using a commercially available kit (Anaspec). After assaying for metabolic activity with AlamarBlue, the caspase 3/7 fluorogenic indicator was added directly to the culture media as indicated by kit instructions. Plates were assayed using a fluorescent plate reader after shaking for 1 hour. Data were expressed as fold increased caspase activity relative to samples receiving no treatment.

The specificity of *plk1* knockdown activity through p53-mediated apoptosis was examined by treating a subset of *plk1*-knockdown cells with a p53 inhibitor, pifithrin α. Reversion to doxorubicin resistance was monitored using the AlamarBlue assay, as described above, comparing doxorubicin sensitization of ternary complex-mediated *plk1* deficient NCI/ADR-RES and OVCAR8 cells in the presence and absence of 5 μM pifithrin α, which was contained within the media for the duration of the experiment. Cell viability (%) was determined by comparing fluorescence of samples to controls and IC_{50} (inhibitory concentration to 50% of the population) was determined.

2.6. Synthesis, loading, and utilization of doxorubicin-loaded micelles for dual delivery with siRNA

pDbB was synthesized and purified as described in Section 2.2 but with an increased molecular weight of the butyl block to 4,400 g/mol (pDbB = 11,700 g/mol (M_n), polydispersity = 1.4) by increasing the polymerization time to 16 hours. This was done to ensure stable doxorubicin loading into the micelle core. Micelles were formed as detailed in Section 2.3 and loaded with doxorubicin using solvent evaporation. Briefly, an 8.6 mM solution of doxorubicin in chloroform was prepared by stirring with a 3-fold molar excess of triethylamine (TEA) in chloroform for 2.5 hours at room temperature. The doxorubicin loading solution was then added to stirring micelle solution (~2 mg/ml) in H_2O, maintaining the overall mixture below 7% v/v chloroform. The chloroform was removed by evaporation, causing doxorubicin to partition into the hydrophobic butyl core. Free doxorubicin was separated from the doxorubicin-micelle solutions using Vivaspin centrifuge filters (MWCO = 30 kDa, PES, Sartorius). The doxorubicin loaded micelles were rinsed three times using nanopure H_2O. Following centrifugation, the purified micelles were resuspended in H_2O and lyophilized. The loading of doxorubicin was determined by resuspending micelles in H_2O and measuring absorbance at 485 nm. By comparing the absorbance of the micelle solution versus a standard curve of free doxorubicin, the weight percent of doxorubicin in the loaded micelle was calculated. Loaded micelles were characterized for size and charge, as discussed in Section 2.3.

The loaded micelles were utilized for dual delivery of siRNA and doxorubicin. Cells (OVCAR8 and NCI/ADR-RES) were plated at 25,000 cells/cm^2. After 24 hours, ternary complexes (both unloaded and loaded with doxorubicin) with micelle charge ratios of 8:1 and overall charge ratios of 2:1 were used to deliver *plk1* siRNA at a final concentration of 25 nM. RT-PCR was used to analyze knockdown 48 hours after treatment as detailed in Section 2.5. In addition, cell viability and caspase 3/7 upregulation were monitored to compare treatments of free doxorubicin, ternary complexes with free doxorubicin, and dually-loaded ternary complexes. For the dually-loaded ternary complexes, cells were exposed to a final doxorubicin concentration of 0.2 μg/ml doxorubicin. The doxorubicin dose for dually-loaded complexes was limited by the loading capacity of the micelles and the ternary complex dose required to maintain the *plk1* siRNA concentration at 25 nM.

2.6. Statistical methods

ANOVA was used to test for treatment effects, and Tukey's test was used for post hoc pairwise comparisons between individual treatment groups.

3. Results and Discussion

3.1 Ternary complex formation and characterization

Reversible addition fragmentation chain transfer (RAFT) polymerization was used to synthesize the diblock copolymer pDbB used to formulate cationic micelles and the pH-responsive polymer pSMA using two-step procedures as shown in Scheme 1. The first block of the pDbB copolymers consisted of poly(dimethylaminoethyl methacrylate) (pDMAEMA), which has been shown to effectively condense nucleic acid drugs [33, 38, 54]. This polymer was used as a macroCTA for the synthesis of the second block, poly(butyl methacrylate). The resulting pDbB copolymers are capable of self-assembling in aqueous environments to form micelles with cationic coronas, as depicted in Figure 1A. Figure 1B shows the particle size and zeta potential of these micelles in PBS at pH 7.4. The naked pDbB micelles were found to have effective diameters of 37 nm and positive zeta potentials of 8.4 mV. Agarose gel shift assays showed that these micelles completely complexed siRNA at micellar charge ratios above 1:1 (Supplementary Information). Formation of binary complexes between siRNA and the pDbB cationic micelles resulted in smaller and more reproducible complexes (35 ± 0.4 nm, Figure 1B) than could be achieved using pDMAEMA homopolymers (356 ± 54 nm, data not shown). Subsequently, these micelles were used as cores for the formation of ternary complexes with siRNA and pH-responsive, membrane disruptive pSMA polymers, as depicted in Figure 1A.

Previously, alkylamine derivatives of pSMA were shown to cause membrane destabilization in response to lowered pH values characteristic of the endosomal/lysosomal pathway[55]. The amount of membrane disruption and the nature of the pH response could be controlled by altering the type and extent of alkylamine modification of the parent pSMA backbone, as well as its molecular weight. Increasing the size of the polymer or changing the extent or type of alkylamine modification of the pSMA backbone to introduce more hydrophobicity generally increased the membrane destabilization caused by the modified pSMA [55]. Based on this work, a 48,500 g/mol pSMA polymer in which 60% of the anhydride groups had been opened with pentylamine was synthesized as shown in Scheme 1, a composition selected to maximize endosomal membrane disruption while limiting polymer size to minimize concerns regarding polymer clearance in potential *in vivo* applications. Recently, Yessine et al. used a similar pH-responsive polymer based on poly(methacrylic acid) in ternary complexes with diblock copolymer micelles to escape lysosomal trafficking and deliver antisense oligodeoxynucleotides to the cytosol of macrophages [65].

Formulation of the ternary complexes is governed by two interrelated charge ratios (Figure 1A). The micelle charge ratio is defined as the ratio of positively-charged DMAEMA residues in the pDbB micelle corona to negatively-charged phosphate groups in the siRNA backbone. Based on published reports of the DMAEMA pKa [64], the degree of protonation of the pDbB corona was assumed to be 50%. The overall charge ratio accounts for the ratio of positive charges from the pDbB micelles to the total negative charges present from both siRNA and pSMA, based on the previously published pKa values for pSMA[55]. Ternary complexes were formulated using micellar charge ratios from 8:1 to 2:1 and overall charge ratios of 4:1, 2:1, and 1.3:1. The minimum micelle charge ratio was the charge ratio necessary to obtain complete siRNA complexation based on gel retardation (see Supplementary Figure 1). The overall charge ratio is defined as the total +:- charge ratio of the ternary complex and the range of accessible overall charge ratios is limited by the micelle charge ratio. The highest possible overall charge ratio is the same as the micelle charge ratio for a ternary complex containing no pSMA. As the amount of anionic pSMA added to the ternary complex increases, neutrality is approached, and pSMA no longer electrostatically interacts with the complexes. Therefore, the theoretical lower limit of the overall charge ratio is unity, but a slightly positive charge ratio is preferential to address concerns of particle stability and cellular uptake. The lowest overall charge ratio employed in this study was 1.3:1. Overall charge ratios throughout the possible range were tested to determine the complex formulation that best optimized particle size, charge, uptake and siRNA delivery. Figure 1B shows zeta potentials for ternary complexes with a fixed micellar charge ratio of 8:1 and overall charge ratios of 4:1, 2:1, 1.3:1 and also for micellar charge ratios of 8:1, 4:1, and 2:1 at a fixed overall charge ratio of 1.3:1. Zeta potentials were found to be similar and slightly positive for all formulations tested (~0.1 mV, with a range of 0 to 1.2 mV, Figure 1B). Although the charge ratios differ for the particles with micelle charge ratio of 8:1 as the overall charge ratio is decreased from 4:1 to 1.3:1, no alteration in surface charge is observed as measured by zeta potential. This is likely due to salt shielding effects from the buffering system utilized for the measurements (Dulbecco's PBS). Despite this effect, this buffer is relevant for such measurements as it is similar in salt concentration and buffering capacity to environments experienced *in vitro* and *in vivo*. Across the range of compositions tested, the particles appear to have slightly positive zeta potentials, which contribute to colloidal stability and should favor endocytotic uptake.

Particle size is an important variable for cellular uptake and is highly influenced by the pSMA content of the ternary complexes. For ternary complexes at a fixed micelle charge ratio, the overall charge ratio decreases as the amount of anionic pSMA in the ternary complexes increases. This is expected to increase the particle size as increasing amounts of pSMA accumulate in the complexes. In fact, such trends in particle size are observed for ternary complexes formed at a constant micelle charge ratio of 8:1 and overall charge ratios of 4:1, 2:1, and 1.3:1. Particle size increases from ~40 nm to ~100 nm across this range (Figure 1B). A similar trend can be seen by examining the size of ternary complexes formulated at fixed overall charge ratio of 1.3:1 and increasing micelle charge ratios from 2:1 to 8:1. Complex size increases significantly from ~30 nm to ~100 nm (Figure 1B) over this range. The pSMA content of the complexes is also increasing over this range, further supporting the idea that the amount of pSMA included within the complex plays a key role in determining the eventual complex size.

The particle size and surface charge are critical design variables for ensuring efficient uptake. It is generally accepted that positively charged particles have enhanced cellular uptake *in vitro* due to interactions between the particles and the negatively charged cell membrane [66, 67]. Additionally, particle size is an important variable for internalization by endocytosis. Previous studies have shown that ~200 nm is the approximate limit for cellular uptake by macropinocytosis, and particles above this size may not be internalized [68–70]. All

of the ternary complex formulations tested in this study had particle sizes well below 200 nm and exhibited slightly positive zeta potentials (Figure 1B), making them attractive candidates for intracellular delivery of therapeutic siRNA.

3.2 Ternary complex cytotoxicity

The cytotoxicity of the ternary complexes was evaluated by incubating NCI/ADR-RES cells in the presence of ternary complexes (micelle charge ratios of 8:1 and overall charge ratios of 4:1, 2:1, and 1.3:1 as well as micelle charge ratios of 8:1, 4:1, and 2:1 and overall charge ratio of 1.3:1) for 24 hours. Relative cell survival was measured by intracellular lactate dehydrogenase (LDH) activity and is shown in Figure 2. Low cytotoxicity (cell survival >90%) was observed for all formulations tested. This result distinguishes the ternary complex system from many synthetic siRNA delivery systems. Cationic polymers and lipids, including PEI, poly(DMAEMA), N-(2,3-dioleoyloxy)propyl-N,N,N-trimethylammonium chloride (DOTMA), and1,2-dioleoyloxy-3-trimethylammonium propane (DOTAP), have been shown to induce apoptosis and necrosis in a variety of cell lines [39, 40, 48–50], and many commercially available transfection reagents also exhibit very high cytotoxicity. As an example, HiPerFect, a cationic lipid formulation, causes a 50% reduction in cell survival after 24 hours (Figure 2). Previous work has shown that decreasing the molecular weight of cationic polymers used for transfection, or modifying polycations with hydrophilic segments can decrease cell toxicity[71–73], though tradeoffs exist between decreasing toxicity and efficacy. In the ternary complex system, the cationic micelle is electrostatically shielded by pSMA and siRNA, and this shielding may reduce cytotoxic interactions with the cell membrane. Moreover, the pDMAEMA blocks of the pDbB micelles are small compared to many commonly used transfection reagents, and their interaction with cellular components may be significantly different in the micelle corona.

3.3 Ternary complex mediated siRNA uptake and plk1 knockdown

Internalization of siRNA complexes at various micelle and overall charge ratios was investigated using flow cytometry. NCI/ADR-RES cells were exposed to ternary complexes at micelle charge ratio of 8:1 and overall charge ratios of 4:1, 2:1, and 1.3:1 as well as complexes at a micelle charge ratios of 8:1, 4:1, and 2:1 at an overall charge ratio of 1.3:1, and the resulting cell uptake is shown in Figure 3A. As expected based on size and charge data, all ternary complexes mediated significant siRNA uptake. There was no correlation of uptake with respect to alterations in overall charge ratio when the micelle charge ratio is fixed at 8:1 (>70% positive cells for all treatments). However, as micelle charge ratio reduces from 8:1 to 2:1 with the overall charge ratio constant at 1.3:1, there is a reduction of FAM-positive cells. At micelle charge ratios of 2:1 and overall charge ratios of 1.3:1, only 24% of cells are positive for siRNA. This reduction might be due to a lesser amount of pH-responsive polymer pSMA in the complexes with the lowest micelle charge ratio. Given that these ternary complexes are ~40 nm and should be endocytosed readily, it is possible that reduced endosomolytic efficacy as a result of decreased pSMA content in the complex may lead to increased extracellular clearance of siRNA through endosomal recycling pathways. Compared with the commercially available carrier HiPerFect, the ternary complexes generally elicit nearly 2-fold greater siRNA-positive cells at the timepoint tested (1 hour). The high percentage of FAM positive cells following treatment with the ternary complexes is significant, since heterogeneous transfection of a cell population and subsequent deviations in gene knockdown may confound the results of *in vitro* experiments[74] and would also have implications for *in vivo* applications, particularly in the case of chemotherapeutic sensitization.

The impact of ternary complex formulation on siRNA transfection efficiency was determined in knockdown experiments against polo-like kinase 1 (*plk1*) using ternary

complexes. Knockdown efficiency was evaluated in both drug sensitive (OVCAR8) and multidrug resistant (NCI/ADR-RES) ovarian cancer cell lines after performing western blots analysis to verify similar levels of constitutive plk1 protein production in the two lines (Supplementary Information). *Plk1* mRNA levels were evaluated using RT-PCR 48 hours after treatment with the complexes. *Plk1* knockdown was evaluated as a function of varying overall charge ratios at a fixed micelle charge ratio. Cells were treated with ternary complexes at a fixed micelle charge ratio of 8:1 and overall charge ratios of 4, 2, and 1.3:1 and *plk1* expression was observed to decrease to ~50% of control, with no statistically significant differences between the treatments (see Supplementary Data). In contrast to this result, *plk1* knockdown is found to decrease as the micelle charge ratio decreases from 8:1 to 4:1 to 2:1 at a fixed overall charge ratio of 1.3:1 (Figure 3B). Though the majority of the data presented in this paper is presented at an overall charge ratio of 2:1, an overall charge ratio of 1.3:1 was employed since this formulation allowed for 3 different micelle charge ratios to be tested. As described in Section 3.1, the ternary complex overall charge ratio is limited by micelle charge ratio, as the addition of anionic pSMA reduces the overall charge ratio. As neutrality is approached, pSMA no longer electrostatically interacts with the complexes. Therefore, the overall charge ratio with the greatest attainable range of micelle charge ratios is 1.3:1. Overall charge ratios of 2:1, show similar trends at micelle charge ratios of 8:1 and 4:1 respectively (data not shown). Figure 3B shows that relative *plk1* expression is reduced to ~52% of control at a micelle charge ratio of 8:1 and overall charge ratio of 1.3:1. Knockdown is reduced as the micelle charge ratio decreases to 4:1 and 2:1, where gene expression is 70% and 85% of control. Similar levels of *plk1* knockdown are apparent in the OVCAR8 and NCI/ADR-RES cells. These results suggest that the micelle charge ratio plays a critical role in siRNA transfection efficiency that is not related to surface charge phenomenon, as each of the complexes was formulated at identical overall charge ratios. At a fixed charge ratio, the micelle charge ratio controls the amount of membrane-disruptive pSMA in the ternary complex. Decreasing knockdown with decreasing micelle charge ratio therefore indicates pSMA plays a critical role in mediating successful siRNA delivery. Based on uptake data, the amount of pSMA impacts the fraction of siRNA positive cells, and the extent of *plk1* knockdown increases with the amount of pSMA, indicating the pSMA content of the complexes plays a critical role in determining the efficiency of siRNA delivery. These results, taken together, indicate that the most potent siRNA knockdown is mediated by particles with micellar charge ratios of 8:1 and overall charge ratios of 4:1, 2:1, or 1.3:1 (not statistically different, see Supplementary Figure 3). The ternary complex composition with an overall charge ratio of 2:1, however, was utilized for all subsequent experimentation.

A siRNA dose response study was performed using ternary complexes at a micelle charge ratio of 8:1 and an overall charge ratio of 2:1. Although there was little response in *plk1* gene expression at 5 nM siRNA, expression was reduced to 70%, 50%, and 40% at 10, 25, and 50 nM siRNA in OVCAR8 cells. Similar reductions in *plk1* expression were also seen using NCI/ADR-RES cells. In addition, a control siRNA (Control siRNA #1, Ambion) was delivered to cells using the ternary complex system at 50 nM and shown to elicit no non-specific plk1 knockdown (data not shown). The level of knockdown achieved by the ternary carriers is highly significant, but does fall short of the level of knockdown mediated by the commercial siRNA delivery reagent HiPerFect, at both 25 nM (Figure 3B) and 50 nM siRNA (Figure 3C), which reduces gene expression to ~40% and ~25% at these doses, respectively. However, the ternary complexes exhibit dramatically reduced cytotoxicity compared to HiPerFect (Figure 2) and also transfect a higher percentage of the total cell population (Figure 3A), offering distinct advantages for both *in vivo* and *in vitro* applications. Given these advantages, the discrepancy between the knockdown obtained using the ternary system and the knockdown using HiPerFect might arise from mechanistic differences outside the scope of this study. Gene knockdown by siRNA delivery is a

complex process involving: siRNA uptake, both in terms of the percentage of the cell population transfected and the concentration of siRNA achieved per cell; endosomal release of intact siRNA into the cytosol; incorporation of siRNA into the RNA silencing complex, and subsequent mRNA degradation. Therefore, more fundamental studies are required to elucidate how future generations of the ternary complex system can be improved to overcome many of these hurdles.

3.4 plk1 knockdown sensitizes multidrug resistant cells to doxorubicin through p53 signaling

Knockdown of *plk1* was expected to increase the sensitivity of OVCAR8 and NCI/ADR-RES cells to chemotherapeutics. Doxorubicin was added as an adjunct following *plk1* siRNA treatment. Cell death, indicated by reduced metabolic activity, was used to evaluate sensitivity to this common chemotherapeutic, and this data is shown in Figure 4A. Cell death correlated with doxorubicin concentration in both cell types, and cells treated with *plk1* siRNA showed increased sensitivity to doxorubicin. As a result of ternary complex mediated reduction of *plk1* expression alone, cell viability was reduced about 20% versus control cells. With the additional treatment of doxorubicin, the IC_{50} was reduced 10-fold in OVCAR8 cells and 20-fold in NCI/ADR-RES (Figure 4C). Further, *plk1* knockdown in NCI/ADR-RES cells increases sensitivity to doxorubicin to the extent observed in OVCAR8 cells with endogenous *plk1* levels (IC_{50} approximately equivalent at 5 μg/mL), demonstrating the potential for *plk1* knockdown in treatment of drug-resistant carcinomas. These results are similar to previous work by Hussain et al. using liposomes targeted to an epithelial cell adhesion molecule to deliver antisense RNA against *bcl2/xl*, that resulted in a 2.5-fold reduction in the IC_{50} of drug-sensitive breast cancer cells exposed to doxorubicin [24]. Additional work by Wu et al., showed that multidrug resistant breast cancer cells depleted of *mdr1* by siRNA treatment (mediated by Oligofectamine) resulted in a 12-fold IC_{50} reduction after 12 days of exposure to doxorubicin[5]. This work has particular relevance, since the resistant breast cancer cell lines used in these previous studies have recently been re-classified as the drug resistant NCI/ADR-RES ovarian cancer cells used here[75]. Though the reduction in IC_{50} observed by Wu et al. is highly significant, it should be noted that the dose of siRNA employed and time required to observe cell-sensitization were both greater than in the present work (200 vs. 25 nM and 12 days vs. 48 hours, respectively). Finally, in a separate study using two nanoparticle formulations for delivery of paclitaxel and siRNA against *mdr1* in multidrug resistant SKOV3 cells, a 10-fold decrease in IC_{50} was observed compared to cells treated with paclitaxel alone [76]. siRNA treatment of the multidrug resistant cells resulted in paclitaxel sensitivity similar to non-resistant cells, and complete knockdown of *mdr1* was achieved using 100 nM siRNA. In the present study, a 25 nM siRNA dose achieved incomplete silencing of *plk1* (50% of control, Figure 3), but completely restored doxorubicin sensitivity in NCI/ADR-RES cells. Together with the results of our present work, these previous studies demonstrate both the potency of siRNA against *plk1* for reversal of multidrug resistance and the efficacy and promise of the polymeric siRNA delivery system described herein.

In cells treated with ternary complexes against *plk1*, cell death following doxorubicin administration was expected to result from caspase-mediated apoptosis activated by increased p53 activity. Caspases 3 and 7 were monitored in OVCAR8 and NCI/ADR-RES cells treated with both doxorubicin and ternary complexes against *plk1*. Caspases 3/7 are upregulated (Figure 4B) in response to *plk1* knockdown and doxorubicin treatment, up to 3.5-fold in OVCAR8 and 1.5-fold in NCI/ADR-RES cells compared to those receiving no treatment. For doxorubicin treatment alone, caspase activation is not as robust, only 2-fold control in OVCAR8 and 1.1-fold in NCI/ADR-RES at the highest doxorubicin concentration used (100 μg/ml). Additionally, *plk1* knockdown alone mediated a modest increase in

caspase (~1.2-fold of control cells). These results indicate that *plk1* knockdown enhances the effects of doxorubicin by facilitating induction of cell death through the classical mitochondrial apoptosis pathway, mediated by p53 signaling. In previous work using a liposomal delivery system, a 3-fold upregulation of caspase 3 in lung cancer cells was observed after treatment with antisense RNA against *bcl2/xl* and doxorubicin compared to cells treated only with doxorubicin[24]. This observation is similar to our current work in OVCAR8 and NCI/ADR-RES cells, where a 1.5-fold increase in caspase activation was observed as a result of treatment with *plk1* siRNA and doxorubicin compared to treatment with doxorubicin alone.

To confirm the role of p53 signaling in increasing caspase-mediated apoptosis, cells treated with *plk1* siRNA and doxorubicin were exposed to pifithrin α, a specific inhibitor of p53. In NCI/ADR-RES cells, the IC_{50} values determined from this experiment indicated partial reversion to the doxorubicin resistant phenotype as a result of p53 inhibition. The inhibited IC_{50} values of *plk1*-depleted OVCAR8 and NCI/ADR-RES cells increased to 2 and 60 μg/mL respectively (Figure 4C), similar to the IC_{50} values of cells with baseline *plk1* expression. These results clearly indicate that the chemotherapeutic sensitization caused by *plk1* knockdown is specific to the p53 signaling mechanism, consistent with the known role of *plk1* in suppressing pro-apoptotic p53 activity.

3.5 Dual delivery of plk1 siRNA and doxorubicin using ternary system

The cationic micelles used to nucleate the ternary complexes offer opportunities for co-delivery of small molecules and siRNA from a single carrier. Doxorubicin was loaded into the hydrophobic butyl methacrylate core of pDbB micelles to enable dual delivery of siRNA and chemotherapeutic. Micelle loading was found to be 10% doxorubicin by weight. Drug loaded micelles and dually-loaded ternary complexes formed using loaded micelles were slightly larger than their unloaded counterparts. At micelle and overall charge ratios of 8:1 and 2:1 the loaded micelle and dually-loaded ternary complexes were 45 ± 2.2 nm and 58 ± 4.5 nm as compared to 37 ± 1.2 nm and 43 ± 0.2 nm, respectively. The increased size of the drug-loaded micelles and complexes results not only from the doxorubicin loading, but changes in the polymer composition necessary to obtain stable doxorubicin entrapment. The butyl block length of the pDbB polymer was extended slightly (from 2,100 g/mol to 4,400 g/mol), thus increasing slightly the size of both the loaded micelles and ternary complexes.

Ternary complex-mediated knockdown was unaffected by doxorubicin loading (data not shown), resulting in ~58% of control plk1 expression in both OVCAR8 and NCI/ADR-RES cells, similar to the original ternary complexes which resulted in ~50% of control expression (Figure 3B) at the same micelle and overall charge ratios (8:1 and 2:1, respectively). These results indicate that neither the reformulated pDbB core nor loading with doxorubicin adversely impacts the ability of the complexes to mediate transfection. As measures of efficacy and sensitization, cell viability and caspase 3/7 upregulation were monitored for cells treated with ternary complexes and soluble doxorubicin and doxorubicin-loaded ternary complexes and the data are shown in Figures 5A and B. The doxorubicin dose across treatment groups was 0.2 μg/mL in order to match the dose obtained from dually-loaded ternary complexes at a siRNA dose of 25 nM. As shown in Figure 5A, reduction in cell viability (~71% viability) was obtained as a result of drug sensitization when cells were concomitantly treated with siRNA and doxorubicin, regardless of which ternary complex formulation was used. The similar levels of decreased cell viability observed between the two siRNA treatment groups suggest that the availability of doxorubicin is not significantly reduced as a result of loading within the micelle core. Further evidence of drug-sensitization by the dually-loaded ternary complexes is provided by caspase 3/7 upregulation, as shown in Figure 5B. *Plk1* siRNA and doxorubicin treatment in both ternary formulations results in caspase upregulation to 1.5-fold of untreated control cells.

Though these results highlight the potential utility of dual delivery, the effects on caspase activation and cell toxicity are weaker than was previously observed with singly loaded siRNA ternary complexes because of the limited doxorubicin concentration (0.2 μg/mL) that could be delivered from the current dual formulation. Various strategies could be pursued to increase doxorubicin loading, including variations in the composition and block length of the hydrophobic micelle core. However, the effects of these modifications could also adversely impact doxorubicin release from the micelle or siRNA delivery, necessitating a trade-off in optimization of the particle formulation. The vastly different therapeutic dose requirements presented by siRNA and chemotherapeutic agents may prove a significant complication in the development of carriers for dual-delivery, despite ongoing research in this area [59]. For this reason, complimentary delivery of such therapeutics from independent systems 76 may offer distinct clinical advantages compared to single-carrier formulations. Alternatively, other molecules of therapeutic utility present opportunities for investigation, including imaging agents to aid in diagnosis and particle fate analysis [60, 77–79].

Conclusions

Here, we have reported the development of a novel pH-responsive micellar siRNA delivery system. This ternary carrier, composed of cationic micelles formed from pDbB and the pH-responsive polymer pSMA, exhibited favorable size and charge (~30–105 nm and slightly positive), was not cytotoxic, and mediated efficient cell uptake of siRNA. Moreover, siRNA delivery was a function of both micelle charge ratio and overall charge ratio, and knockdown was siRNA concentration-dependent. The optimized formulation resulted in ~50% of control *plk1* gene expression and doxorubicin sensitivity in multidrug resistant NCI/ADR-RES, comparable to the sensitivity of the parental, non-resistant cell lineage, OVCAR8. This phenotypic alteration specifically implicated the p53 signaling pathway, based on upregulation of caspase 3/7 and reversion to the drug-resistant phenotype upon administration of a p53 inhibitor. Doxorubicin was successfully loaded into pDbB micelles used to form ternary complexes capable of dual delivery of chemotherapeutic and siRNA. Dual delivery of siRNA and doxorubicin resulted in less potent cell killing and caspase upregulation than when siRNA and doxorubicin were delivered singularly due to limitations in doxorubicin loading, outlining the complicated needs of a dual-delivery system for siRNA and drug. However, the effectiveness and low cytotoxicity of this new carrier make it a promising candidate for future siRNA delivery studies in disease models and future experiments will involve treatment by doxorubicin and *plk1* siRNA in NCI/ADR-RES xenograft tumor models.

Supplementary Material

Refer to Web version on PubMed Central for supplementary material.

Acknowledgments

The authors gratefully acknowledge the National Institute of Health (EB2991) for funding. Danielle S.W. Benoit is a Merck Fellow supported by the Damon Runyon Cancer Research Foundation (DRG-1948-07).

References

1. Dykxhoorn DM, Novina CD, Sharp PA. Killing the messenger: short RNAs that silence gene expression. Nat. Rev. Mol. Cell Biol 2003;4:457–467. [PubMed: 12778125]
2. Gartel AL, Kandel ES. RNA interference in cancer. Biomol. Eng 2006;23:17–34. [PubMed: 16466964]

3. Lima RT, Martins LM, Guimaraes JE, Sambade C, Vasconcelos MH. Specific downregulation of bcl-2 and xIAP by RNAi enhances the effects of chemotherapeutic agents in MCF-7 human breast cancer cells. Cancer Gene Ther 2004;11:309–316. [PubMed: 15031723]
4. Pichler A, Zelcer N, Prior JL, Kuil AJ, Piwnica-Worms D. In vivo RNA interference-mediated ablation of MDR1 P-glycoprotein. Clin. Cancer Res 2005;11:4487–4494. [PubMed: 15958634]
5. Wu H, Hait WN, Yang JM. Small interfering RNA-induced suppression of MDR1 (P-glycoprotein) restores sensitivity to multidrug-resistant cancer cells. Cancer res 2003;63:1515–1519. [PubMed: 12670898]
6. Hannay JA, Liu J, Zhu QS, Bolshakov SV, Li L, Pisters PW, Lazar AJ, Yu D, Pollock RE, Lev D. Rad51 overexpression contributes to chemoresistance in human soft tissue sarcoma cells: a role for p53/activator protein 2 transcriptional regulation. Mol. Cancer Ther 2007;6:1650–1660. [PubMed: 17513613]
7. Kang HC, Kim IJ, Park HW, Jang SG, Ahn SA, Yoon SN, Chang HJ, Yoo BC, Park JG. Regulation of MDK expression in human cancer cells modulates sensitivities to various anticancer drugs: MDK overexpression confers to a multi-drug resistance. Cancer lett 2007;247:40–47. [PubMed: 16644108]
8. Lillig CH, Lonn ME, Enoksson M, Fernandes AP, Holmgren A. Short interfering RNA-mediated silencing of glutaredoxin 2 increases the sensitivity of HeLa cells toward doxorubicin and phenylarsine oxide. Proc. Natl. Acad. Sci. U S A 2004;101:13227–13232. [PubMed: 15328416]
9. Liu TG, Yin JQ, Shang BY, Min Z, He HW, Jiang JM, Chen F, Zhen YS, Shao RG. Silencing of hdm2 oncogene by siRNA inhibits p53-dependent human breast cancer. Cancer Gene Ther 2004;11:748–756. [PubMed: 15375377]
10. Suzuki A, Toi M, Yamamoto Y, Saji S, Muta M, Takeshi T. Role of MDM2 Overexpression in Doxorubicin Resistance of Breast Carcinoma. Jap. J. Cancer Res 1998;89:221–227. [PubMed: 9548451]
11. Ando K, Ozaki T, Yamamoto H, Furuya K, Hosoda M, Hayashi S, Fukuzawa M, Nakagawara A. Polo-like kinase 1 (Plk1) inhibits p53 function by physical interaction and phosphorylation. J. Biol. Chem 2004;279:25549–25561. [PubMed: 15024021]
12. Strebhardt K, Ullrich A. Targeting polo-like kinase 1 for cancer therapy. Nat. Rev. Cancer 2006;6:321–330. [PubMed: 16557283]
13. Smith MR, Wilson ML, Hamanaka R, Chase D, Kung H, Longo DL, Ferris DK. Malignant transformation of mammalian cells initiated by constitutive expression of the polo-like kinase. Biochem. Biophys. Res. Commun 1997;234:397–405. [PubMed: 9177283]
14. Smits VA, Klompmaker R, Arnaud L, Rijksen G, Nigg EA, Medema RH. Polo-like kinase-1 is a target of the DNA damage checkpoint. Nat. Cell Biol 2000;2:672–676. [PubMed: 10980711]
15. van Vugt MA, Bras A, Medema RH. Polo-like kinase-1 controls recovery from a G2 DNA damage-induced arrest in mammalian cells. Mol. Cell 2004;15:799–811. [PubMed: 15350223]
16. Ahr A, Karn T, Solbach C, Seiter T, Strebhardt K, Holtrich U, Kaufmann M. Identification of high risk breast-cancer patients by gene expression profiling. Lancet 2002;359:131–132. [PubMed: 11809257]
17. Knecht R, Elez R, Oechler M, Solbach C, von Ilberg C, Strebhardt K. Prognostic significance of polo-like kinase (PLK) expression in squamous cell carcinomas of the head and neck. Cancer res 1999;59:2794–2797. [PubMed: 10383133]
18. Knecht R, Oberhauser C, Strebhardt K. PLK (polo-like kinase), a new prognostic marker for oropharyngeal carcinomas. Int. J. Cancer 2000;89:535–536. [PubMed: 11102900]
19. Chen J, Dai G, Wang YQ, Wang S, Pan FY, Xue B, Zhao DH, Li CJ. Polo-like kinase 1 regulates mitotic arrest after UV irradiation through dephosphorylation of p53 and inducing p53 degradation. FEBS Lett 2006;580:3624–3630. [PubMed: 16753148]
20. Gumireddy K, Reddy MV, Cosenza SC, Boominathan R, Baker SJ, Papathi N, Jiang J, Holland J, Reddy EP. ON01910, a non-ATP-competitive small molecule inhibitor of Plk1, is a potent anticancer agent. Cancer Cell 2005;7:275–286. [PubMed: 15766665]
21. Spankuch-Schmitt B, Bereiter-Hahn J, Kaufmann M, Strebhardt K. Effect of RNA silencing of polo-like kinase-1 (PLK1) on apoptosis and spindle formation in human cancer cells. J. Natl. Cancer Inst 2002;94:1863–1877. [PubMed: 12488480]

22. Spankuch-Schmitt B, Wolf G, Solbach C, Loibl S, Knecht R, Stegmuller M, von Minckwitz G, Kaufmann M, Strebhardt K. Downregulation of human polo-like kinase activity by antisense oligonucleotides induces growth inhibition in cancer cells. Oncogene 2002;21:3162–3171. [PubMed: 12082631]

23. Liu X, Erikson RL. Polo-like kinase (Plk)1 depletion induces apoptosis in cancer cells. Proc. Natl. Acad. Sci U S A 2003;100:5789–5794. [PubMed: 12732729]

24. Hussain S, Pluckthun A, Allen TM, Zangemeister-Wittke U. Chemosensitization of carcinoma cells using epithelial cell adhesion molecule-targeted liposomal antisense against bcl-2/bcl-xL. Mol. Cancer Ther 2006;5:3170–3180. [PubMed: 17172421]

25. Chen L, Feng P, Li S, Long D, Cheng J, Lu Y, Zhou D. Effect of hypoxia-inducible factor-1alpha silencing on the sensitivity of human brain glioma cells to doxorubicin and etoposide. Neurochemical res 2009;34:984–990.

26. Ischenko I, Camaj P, Seeliger H, Kleespies A, Guba M, De Toni EN, Schwarz B, Graeb C, Eichhorn ME, Jauch KW, Bruns CJ. Inhibition of Src tyrosine kinase reverts chemoresistance toward 5-fluorouracil in human pancreatic carcinoma cells: an involvement of epidermal growth factor receptor signaling. Oncogene 2008;27:7212–7222. [PubMed: 18794807]

27. Nardinocchi L, Puca R, Sacchi A, D'Orazi G. Inhibition of HIF-1alpha activity by homeodomain-interacting protein kinase-2 correlates with sensitization of chemoresistant cells to undergo apoptosis. Mol. cancer 2009;8:1. [PubMed: 19128456]

28. Sangodkar J, Difeo A, Feld L, Bromberg R, Schwartz R, Huang F, Terzo EA, Choudhri A, Narla G. Targeted reduction of KLF6-SV1 restores chemotherapy sensitivity in resistant lung adenocarcinoma. Lung cancer 2009;66:292–297. [PubMed: 19328586]

29. Singh A, Boldin-Adamsky S, Thimmulappa RK, Rath SK, Ashush H, Coulter J, Blackford A, Goodman SN, Bunz F, Watson WH, Gabrielson E, Feinstein E, Biswal S. RNAi-mediated silencing of nuclear factor erythroid-2-related factor 2 gene expression in non-small cell lung cancer inhibits tumor growth and increases efficacy of chemotherapy. Cancer res 2008;68:7975–7984. [PubMed: 18829555]

30. You H, Jin J, Shu H, Yu B, Milito AD, Lozupone F, Deng Y, Tang N, Yao G, Fais S, Gu J, Qin W. Small interfering RNA targeting the subunit ATP6L of proton pump V-ATPase overcomes chemoresistance of breast cancer cells. Cancer lett 2009;280:110–119. [PubMed: 19299075]

31. Yu L, Wu WK, Li ZJ, Liu QC, Li HT, Wu YC, Cho CH. Enhancement of doxorubicin cytotoxicity on human esophageal squamous cell carcinoma cells by indomethacin and SC236 via inhibiting P-glycoprotein activity. Molecular pharm 2009;75:1364–1373.

32. Aral C, Akbuga J. Preparation and in vitro transfection efficiency of chitosan microspheres containing plasmid DNA:poly(L-lysine) complexes. J. Pharm. Pharm. Sci 2003;6:321–326. [PubMed: 14738712]

33. Ge Q, Filip L, Bai A, Nguyen T, Eisen HN, Chen J. Inhibition of influenza virus production in virus-infected mice by RNA interference. Proc. Natl. Acad. Sci. U S A 2004;101:8676–8681. [PubMed: 15173599]

34. Jiang T, Chang J, Wang C, Ding Z, Chen J, Zhang J, Kang ET. Adsorption of plasmid DNA onto N,N'- (dimethylamino)ethyl-methacrylate graft-polymerized poly-L-lactic acid film surface for promotion of in-situ gene delivery. Biomacromolecules 2007;8:1951–1957. [PubMed: 17472337]

35. Kawano T, Okuda T, Aoyagi H, Niidome T. Long circulation of intravenously administered plasmid DNA delivered with dendritic poly(L-lysine) in the blood flow. J. Control. Release 2004;99:329–337. [PubMed: 15380641]

36. Kim TG, Kang SY, Kang JH, Cho MY, Kim JI, Kim SH, Kim JS. Gene transfer into human hepatoma cells by receptor-associated protein/polylysine conjugates. Bioconj. chem 2004;15:326–332.

37. Shim MS, Kwon YJ. Controlled delivery of plasmid DNA and siRNA to intracellular targets using ketalized polyethylenimine. Biomacromolecules 2008;9:444–455. [PubMed: 18186606]

38. You YZ, Manickam DS, Zhou QH, Oupicky D. Reducible poly(2-dimethylaminoethyl methacrylate): synthesis, cytotoxicity, and gene delivery activity. J. Control. Release 2007;122:217–225. [PubMed: 17574292]

39. Lasic, DD. Liposomes in Gene Delivery. Boca Raton, Fl: CRC Press; 1997.

40. Liu D, Song YK. Cationic liposome-mediated transfection in vivo. Gene. Ther. Mol. Biol 1998;2:59–68.
41. Akinc A, Zumbuehl A, Goldberg M, Leshchiner ES, Busini V, Hossain N, Bacallado SA, Nguyen DN, Fuller J, Alvarez R, Borodovsky A, Borland T, Constien R, de Fougerolles A, Dorkin JR, Narayanannair Jayaprakash K, Jayaraman M, John M, Koteliansky V, Manoharan M, Nechev L, Qin J, Racie T, Raitcheva D, Rajeev KG, Sah DW, Soutschek J, Toudjarska I, Vornlocher HP, Zimmermann TS, Langer R, Anderson DG. A combinatorial library of lipid-like materials for delivery of RNAi therapeutics. Nat. Biotechnol 2008;26:561–569. [PubMed: 18438401]
42. Grimm D, Kay MA. From virus evolution to vector revolution: use of naturally occurring serotypes of adeno-associated virus (AAV) as novel vectors for human gene therapy. Curr. Gene Ther 2003;3:281–304. [PubMed: 12871018]
43. Hughson FM. Structural characterization of viral fusion proteins. Curr. Biol 1995;5:265–274. [PubMed: 7780737]
44. Morrissey DV, Lockridge JA, Shaw L, Blanchard K, Jensen K, Breen W, Hartsough K, Machemer L, Radka S, Jadhav V, Vaish N, Zinnen S, Vargeese C, Bowman K, Shaffer CS, Jeffs LB, Judge A, MacLachlan I, Polisky B. Potent and persistent in vivo anti-HBV activity of chemically modified siRNAs. Nat. Biotechnol 2005;23:1002–1007. [PubMed: 16041363]
45. Plank C, Oberhauser B, Mechtler K, Koch C, Wagner E. The influence of endosome-disruptive peptides on gene transfer using synthetic virus-like gene transfer systems. J. Biol. Chem 1994;269:12918–12924. [PubMed: 8175709]
46. Skehel JJ, Wiley DC. Receptor binding and membrane fusion in virus entry: the influenza hemagglutinin. Annu. Rev. Biochem 2000;69:531–569. [PubMed: 10966468]
47. Zimmermann TS, Lee AC, Akinc A, Bramlage B, Bumcrot D, Fedoruk MN, Harborth J, Heyes JA, Jeffs LB, John M, Judge AD, Lam K, McClintock K, Nechev LV, Palmer LR, Racie T, Rohl I, Seiffert S, Shanmugam S, Sood V, Soutschek J, Toudjarska I, Wheat AJ, Yaworski E, Zedalis W, Koteliansky V, Manoharan M, Vornlocher HP, MacLachlan I. RNAi-mediated gene silencing in non-human primates. Nature 2006;441:111–114. [PubMed: 16565705]
48. Hunter AC. Molecular hurdles in polyfectin design and mechanistic background to polycation induced cytotoxicity. Adv. Drug Deliv. Rev 2006;58:1523–1531. [PubMed: 17079050]
49. Jones RA, Poniris MH, Wilson MR. pDMAEMA is internalised by endocytosis but does not physically disrupt endosomes. J. Control. Release 2004;96:379–391. [PubMed: 15120895]
50. Kim DH, Rossi JJ. Strategies for silencing human disease using RNA interference. Nat. Rev. Genet 2007;8:173–184. [PubMed: 17304245]
51. El-Sayed ME, Hoffman AS, Stayton PS. Rational design of composition and activity correlations for pH-responsive and glutathione-reactive polymer therapeutics. J. Control. Release 2005;104:417–427. [PubMed: 15984055]
52. Jones RA, Cheung CY, Black FE, Zia JK, Stayton PS, Hoffman AS, Wilson MR. Poly(2-alkylacrylic acid) polymers deliver molecules to the cytosol by pH-sensitive disruption of endosomal vesicles. Biochem. J 2003;372:65–75. [PubMed: 12583812]
53. Stayton PS, El-Sayed ME, Murthy N, Bulmus V, Lackey C, Cheung C, Hoffman AS. 'Smart' delivery systems for biomolecular therapeutics. Orthod. Craniofac. Res 2005;8:219–225. [PubMed: 16022724]
54. Convertine AJ, Benoit DSW, Duvall CL, Hoffman AS, Stayton PS. Development of a novel endosomolytic diblock copolymer for siRNA delivery. J. Control. Release 2009;133:221–229. [PubMed: 18973780]
55. Henry SM, El-Sayed ME, Pirie CM, Hoffman AS, Stayton PS. pH-responsive poly(styrene-alt-maleic anhydride) alkylamide copolymers for intracellular drug delivery. Biomacromolecules 2006;7:2407–2414. [PubMed: 16903689]
56. Guo W, Lee RJ. Efficient gene delivery using anionic liposome-complexed polyplexes (LPDII). Bioscience reports 2000;20:419–432. [PubMed: 11332603]
57. Kusonwiriyawong C, van de Wetering P, Hubbell JA, Merkle HP, Walter E. Evaluation of pH-dependent membrane-disruptive properties of poly(acrylic acid) derived polymers. Eur. J. Pharm. Biopharm 2003;56:237–246. [PubMed: 12957638]

58. Nomura T, Saikawa A, Morita S, Sakaeda Kakutani T, Yamashita F, Honda K, Takakura Y, Hashida M. Pharmacokinetic characteristics and therapeutic effects of mitomycin C-dextran conjugates after intratumoural injection. J. Control. Release 1998;52:239–252. [PubMed: 9743445]
59. Qiu LY, Bae YH. Self-assembled polyethylenimine-graft-poly(epsilon-caprolactone) micelles as potential dual carriers of genes and anticancer drugs. Biomaterials 2007;28:4132–4142. [PubMed: 17582489]
60. Rodriguez VB, Henry SM, Hoffman AS, Stayton PS, Li X, Pun SH. Encapsulation and stabilization of indocyanine green within poly(styrene-alt-maleic anhydride) block-poly(styrene) micelles for near-infrared imaging. J. Biomed. Opt 2008;13:014025. [PubMed: 18315383]
61. Moad G, Chong YK, Postma A, Rizzardo E, Thang SH. Advances in RAFT polymerization: the synthesis of polymers with defined end-groups. Polymer 2005;46:8458–8468.
62. Mitsukami Y, Donovan MS, Lowe AB, McCormick CL. Water-soluble polymers. 81. Direct synthesis of hydrophilic styrenic-based homopolymers and block copolymers in aqueous solution via RAFT. Macromolecules 2001;34:2248–2256.
63. Sahlin S, Hed J, Rundquist I. Differentiation between attached and ingested immune complexes by a fluorescence quenching cytofluorometric assay. J. Immunol. Methods 1983;60:115–124. [PubMed: 6406600]
64. Patrickios CS, Hertler WR, Hatton TA. Protein complexation with acrylic polyampholytes. Biotechnol. Bioeng 1994;44:1031–1039. [PubMed: 18623019]
65. Yessine MA, Dufresne MH, Meier C, Petereit HU, Leroux JC. Proton-actuated membrane-destabilizing polyion complex micelles. Bioconj. chem 2007;18:1010–1014.
66. Grayson AC, Doody AM, Putnam D. Biophysical and structural characterization of polyethylenimine-mediated siRNA delivery in vitro. Pharm. Res 2006;23:1868–1876. [PubMed: 16845585]
67. Segura T, Hubbell JA. Synthesis and in vitro characterization of an ABC triblock copolymer for siRNA delivery. Bioconj. chem 2007;18:736–745.
68. Bishop NE. An Update on Non-clathrin-coated Endocytosis. Rev. Med. Virol 1997;7:199–209. [PubMed: 10398484]
69. Oupicky D, Carlisle RC, Seymour LW. Triggered intracellular activation of disulfide crosslinked polyelectrolyte gene delivery complexes with extended systemic circulation in vivo. Gene Ther 2001;8:713–724. [PubMed: 11406766]
70. Rejman J, Oberle V, Zuhorn IS, Hoekstra D. Size-dependent internalization of particles via the pathways of clathrin- and caveolae-mediated endocytosis. Biochem. J 2004;377:159–169. [PubMed: 14505488]
71. Lee Y, Mo H, Koo H, Park JY, Cho MY, Jin GW, Park JS. Visualization of the degradation of a disulfide polymer, linear poly(ethylenimine sulfide), for gene delivery. Bioconj. chem 2007;18:13–18.
72. Neu M, Fischer D, Kissel T. Recent advances in rational gene transfer vector design based on poly(ethylene imine) and its derivatives. J. Gene. Med 2005;7:992–1009. [PubMed: 15920783]
73. vandeWetering P, Cherng JY, Talsma H, Hennink WE. Relation between transfection efficiency and cytotoxicity of poly(2-(dimethylamino)ethyl methacrylate)/plasmid complexes. J. Control. Release 1997;49:59–69.
74. Chen AA, Derfus AM, Khetani SR, Bhatia SN. Quantum dots to monitor RNAi delivery and improve gene silencing. Nucleic Acids Res 2005;33:e190. [PubMed: 16352864]
75. Liscovitch M, Ravid D. A case study in misidentification of cancer cell lines: MCF-7/AdrR cells (re-designated NCI/ADR-RES) are derived from OVCAR-8 human ovarian carcinoma cells. Cancer lett 2007;245:350–352. [PubMed: 16504380]
76. Yadav S, van Vlerken LE, Little SR, Amiji MM. Evaluations of combination MDR-1 gene silencing and paclitaxel administration in biodegradable polymeric nanoparticle formulations to overcome multidrug resistance in cancer cells. Cancer chemo. pharm 2009;63:711–722.
77. Blanco E, Kessinger CW, Sumer BD, Gao J. Multifunctional micellar nanomedicine for cancer therapy. Exp. biol. med 2009;234:123–131.

78. Santra S, Kaittanis C, Grimm J, Perez JM. Drug/Dye-Loaded, Multifunctional Iron Oxide Nanoparticles for Combined Targeted Cancer Therapy and Dual Optical/Magnetic Resonance Imaging. Small 2009;5:1862–1868. [PubMed: 19384879]

79. Sumer B, Gao J. Theranostic nanomedicine for cancer. Nanomedicine 2008;3:137–140. [PubMed: 18373419]

A

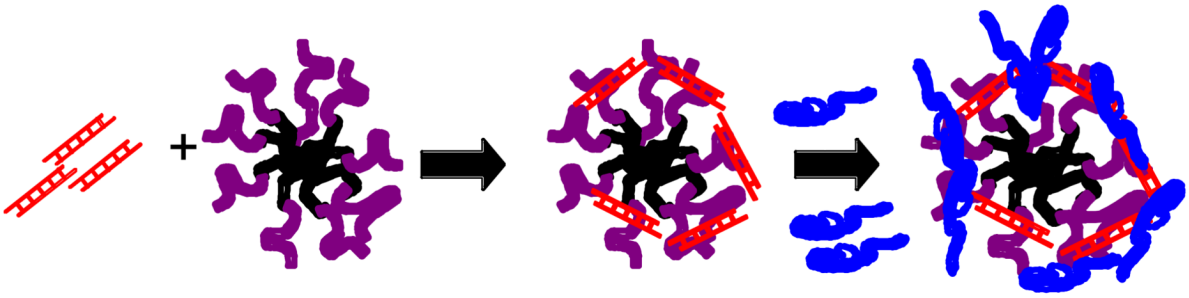

B

Charge Ratio		Diameter (nm) ± Standard Error	Zeta Potential (mV) ± Standard Error
Micelle (+/-)	Overall (+/-)		
pDbB micelle		37 ± 1.2	8.4 ± 2.6
8:1 + siRNA		35 ± 0.4	0.5 ± 1.0
8:1	4:1	43 ± 0.2	0.4 ± 0.4
8:1	2:1	103 ± 6.3	1.2 ± 3.7
8:1	1.3:1	95 ± 5.8	0 ± 0.6
4:1	1.3:1	40 ± 7.5	0.4 ± 0.5
2:1	1.3:1	34 ± 4.1	0.4 ± 0.8

Figure 1. Ternary complex formation and characterization

(A) Depiction of ternary complex formation including micelle charge ratio and overall charge ratio and (B) ternary complex characterization with respect to size and surface charge. (A) The diblock pDbB is shown in purple for poly(DMAEMA) and black for poly(butyl methacrylate), and siRNA is depicted in red. The pH-responsive polymer pSMA is shown in blue. Two charge ratios govern complex formation. The **micelle** charge ratio is defined as the ratio of positively-charged DMAEMA residues in the pDbB micelle corona to negatively-charged phosphate groups in the siRNA backbone. Based on published reports of the pDMAEMA pKa [64], the degree of protonation of the pDMAEMA corona was assumed to be 50%. The **overall** charge ratio accounts for the ratio of positive charges from the pDbB micelles to the total negative charges present from both siRNA and pSMA, based on the previously published pKa values for pSMA[55]. (B) Micelles, micelles+siRNA, and ternary complexes were formed at various micellar and overall charge ratios at 25 nM siRNA concentrations in phosphate buffered saline and characterized for size and zeta potential using a ZetaPALS detector. Data are from three independent experiments conducted in triplicate.

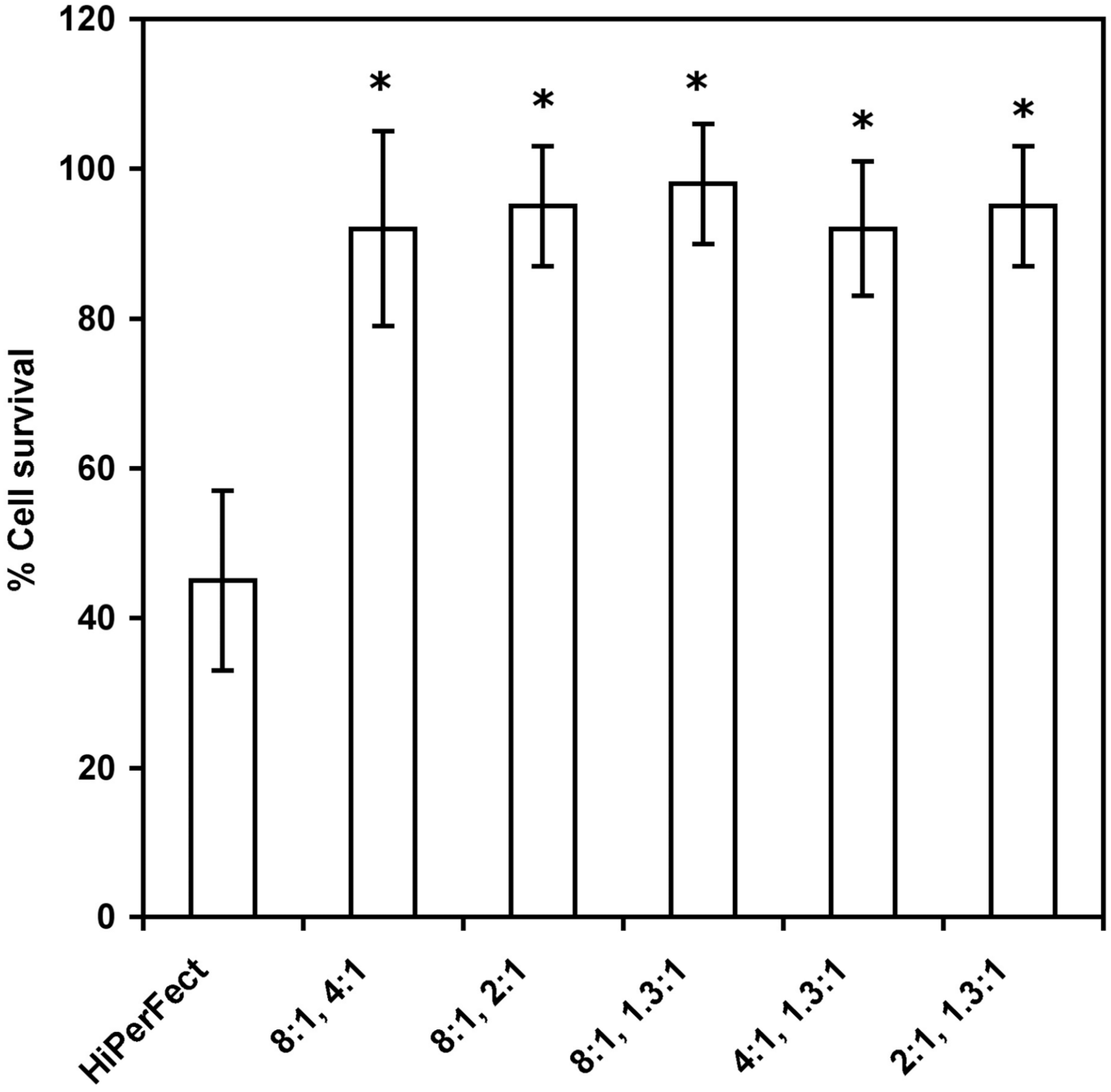

Figure 2. Ternary complex cytotoxicity as a function of ternary carrier composition

NCI/ADR-RES cells were treated with siRNA (Negative control #1) at 25 nM using ternary complexes at various micelle charge ratios (listed first) and overall charge ratios (listed second). After 24 hours, cell lysate was collected and assayed for lactate dehydrogenase, a measure of cell viability, and data is shown relative to untreated cells. Data are from three independent experiments conducted in triplicate with error bars representing standard deviation. Statistical significance was evaluated at a level of $p < 0.05$ with the following symbols * indicating significance versus HiPerFect.

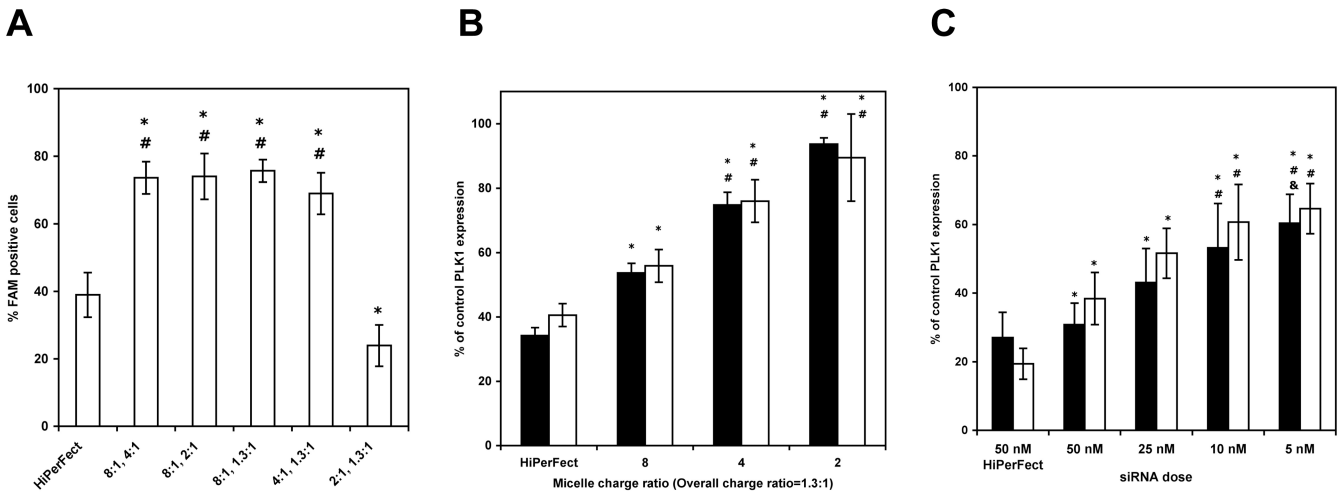

Figure 3. Ternary complex mediated siRNA uptake and *plk1* knockdown

FAM-labeled siRNA uptake by NCI/ADR-RES cells was measured using flow cytometry 1 hour after treatment (A). *Plk1* knockdown in OVCAR8 (black) and NCI/ADR-RES (white) cells was measured using real time RT-PCR 48 hours after treatment with ternary complexes as a function of micelle charge ratio with overall charge ratio fixed at 1.3:1 (B), and siRNA dose (5–50 nM). A commercially available transfection reagent, HiPerFect (Qiagen), was used as a positive control. For A, statistical significance was evaluated at a level of $p < 0.05$ with the following symbols indicating significance versus HiPerFect and treatments with micelle charge ratios of 2:1 and overall charge ratios of 1.3:1, respectively: *, #. For B, statistical significance was evaluated at a level of $p < 0.05$ with the following symbols indicating significance versus treatments of HiPerFect and micelle charge ratios of 8:1, respectively: *, #. For C, statistical significance was evaluated at a level of $p < 0.05$ with the following symbols indicating statistical significance versus treatments of 50 nM siRNA with HiPerFect, 50 nM siRNA with the ternary delivery system, and 25 nM siRNA with the ternary delivery system, respectively: *, #, and &.

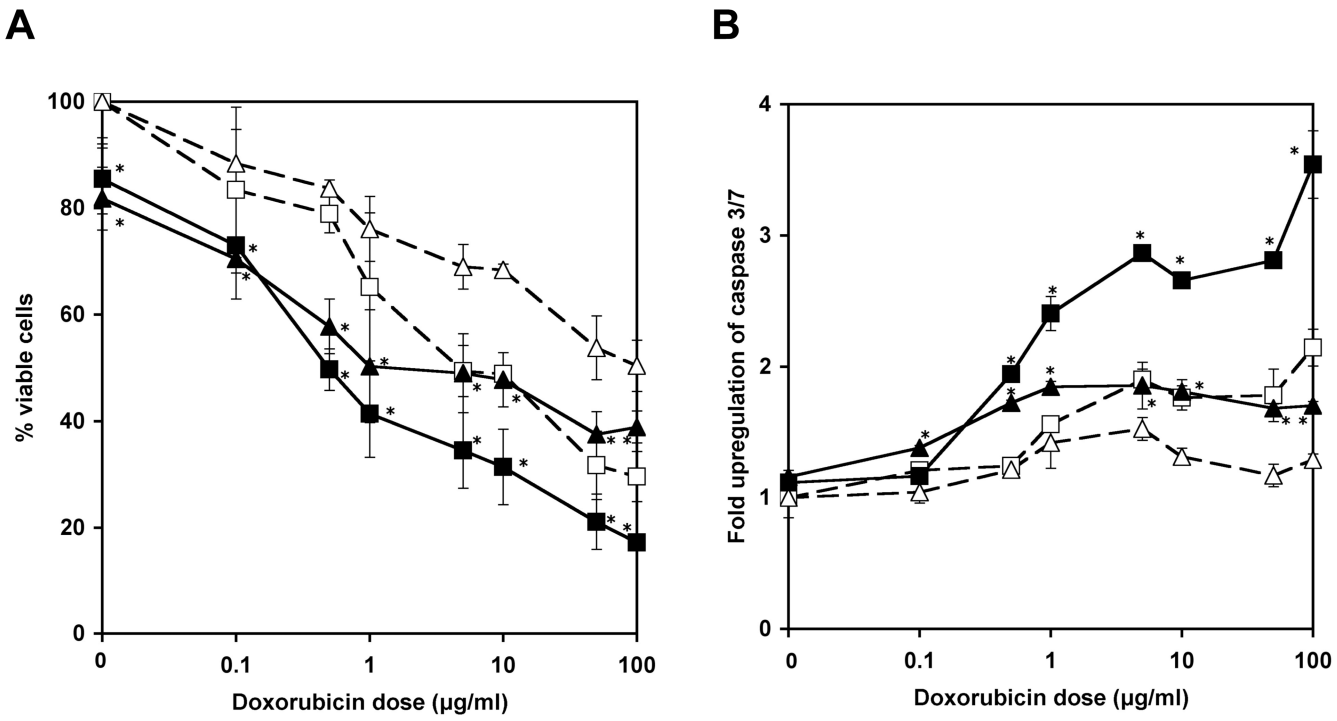

C

	IC_{50} (μg/mL)	Fold Sensitization	IC_{50} (μg/mL) + p53 inhibitor
OVCAR8	5 ± 0.6	-	-
OVCAR8+plk1 siRNA	0.5 ± 0.1	10	2 ± 0.5
NCI/ADR-RES	100 ± 13	-	-
NCI/ADR-RES+plk1 siRNA	5 ± 0.8	20	60 ± 12

Figure 4. *plk1* knockdown sensitizes multidrug resistant cells to doxorubicin through p53 signaling

OVCAR8 and NCI/ADR-RES were treated with *plk1* siRNA ternary complexes and doxorubicin (--□--; OVCAR8 (no doxorubicin), –■–; OVCAR8 + doxorubicin, --Δ--; NCI/ADR-RES (no doxorubicin), –▲–; NCI/ADR-RES + doxorubicin. Resulting % viable cells (A) and caspase 3/7 upregulation (B) was assessed and expressed compared to untreated cells (as a percent in A or as a fold-upregulation in B). IC_{50} values were extrapolated from A and listed in C. In addition, a p53 inhibitor, pifithrin α was added to the cells in addition to doxorubicin and resulting IC_{50} values from those experiments are listed in C. Representative data ± standard deviations are shown from 3 independent studies done in quadruplicate. Statistical significance was evalulated at a level of $p < 0.05$ with * indicating significance versus cells without siRNA delivery at the same doxorubicin concentrations. IC_{50} values were extrapolated from A and listed in C. In addition, a p53 inhibitor, pifithrin α was added to the cells in addition to doxorubicin and resulting IC_{50} values from those experiments are listed in C. Representative data ± standard deviations are shown from 3 independent studies done in quadruplicate.

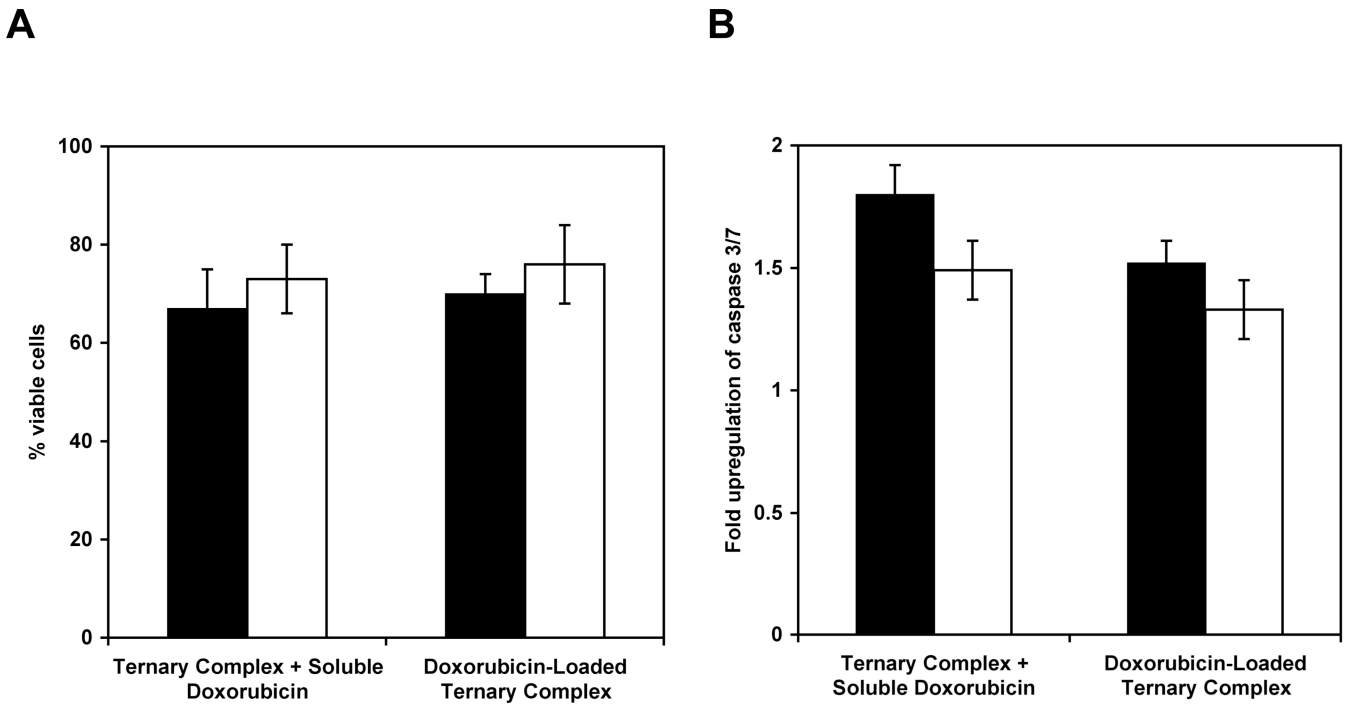

Figure 5. Doxorubicin-loaded ternary complexes are effective at initiating loss of cell viability and upregulated caspase 3/7 levels

OVCAR8 (black bars) and NCI/ADR-RES (white bars) were treated with dually-loaded *plk1* siRNA and doxorubicin ternary complexes. Resulting cell viability (A) and caspase 3/7 upregulation (B) was assessed and expressed compared to untreated cells (as a percent in A or as a fold-upregulation in B). The doxorubicin dose was 0.2 μg/mL across treatments and experimental conditions. Statistical significance was tested, however there were no differences $p > 0.05$ between the two treatments, ternary complex-delivered plk1 siRNA and soluble doxorubicin and doxorubicin-loaded ternary complex delivered plk1 siRNA.

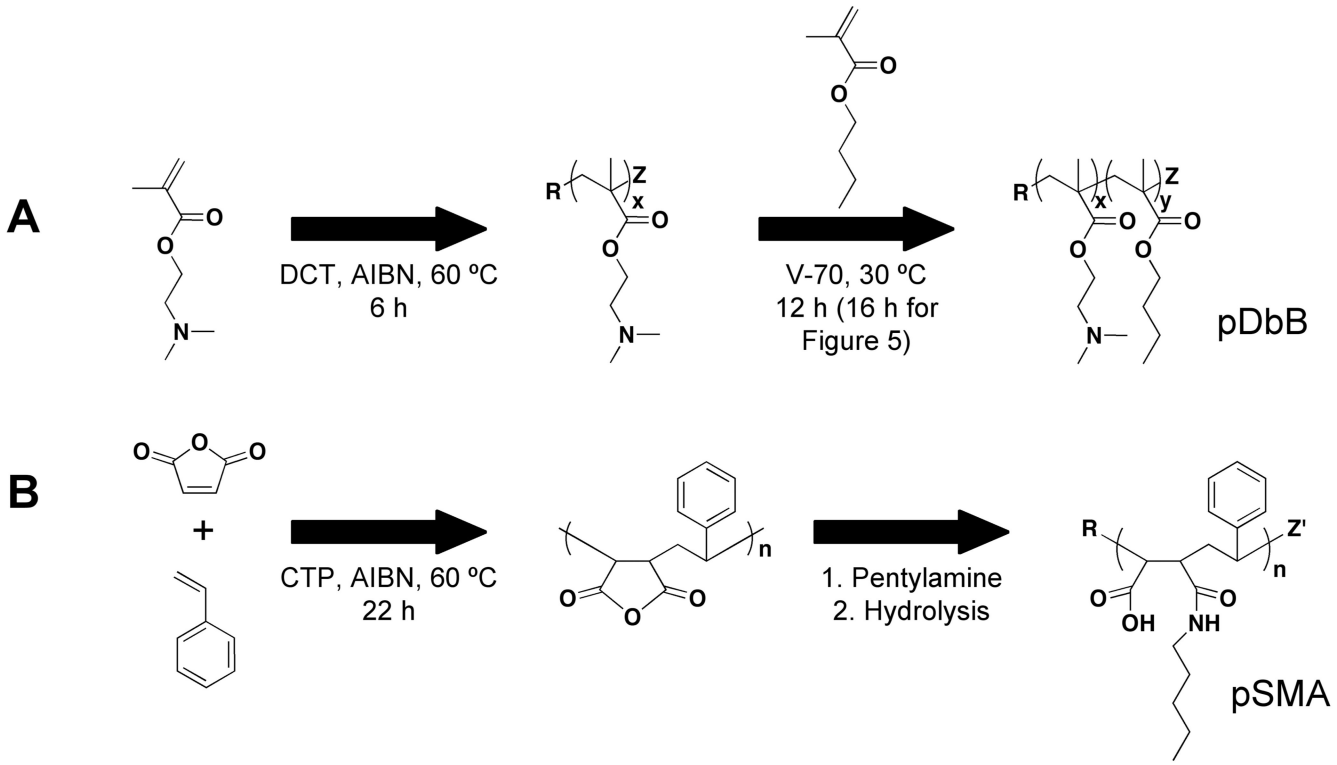

Scheme 1. Polymer Synthesis

(A) Synthesis of the diblock polymer pDbB *via* a two step RAFT polymerization. (B) A pH-sensitive derivative of pSMA was obtained by RAFT polymerization followed by subsequent reactions to modify 60% of the anhydride groups with pentylamine. R = $CCNCH_3C_2H_4CO_2H$, Z = $SCSSC_{12}H_{25}$, x ~ 46, y ~ 15 (~ 31 for Figure 5), Z' = $SCSC_6H_5$ n ~ 190.